

Article

# A Pseudopeptide Polymer Micelle Used for Asymmetric Catalysis of the Aldol Reaction in Water

Keyuan Liu, Long Ye, Yao Wang, Ganhong Du and Liming Jiang \* 

MOE Key Laboratory of Macromolecular Synthesis and Functionalization, Department of Polymer Science and Engineering, Zhejiang University, Hangzhou 310027, China; lkychem@zju.edu.cn (K.L.); 21529010@zju.edu.cn (L.Y.); 21329021@zju.edu.cn (Y.W.); duganhong@zju.edu.cn (G.D.)

\* Correspondence: cejlm@zju.edu.cn

Received: 12 August 2018; Accepted: 5 September 2018; Published: 10 September 2018



**Abstract:** Micelles assembled from amphiphilic molecules have proved to be ideal scaffolds to construct artificial catalysts mimicking enzymatic catalytic behavior. In this paper, we describe the synthesis of amphiphilic poly(2-oxazoline) derivatives with L-prolinamide units in the side chain and their application in asymmetric aldol reactions. Upon dissolution in water, the pseudopeptide polymers self-assembled into particles with different sizes, relying on the copolymer composition and distribution of hydrophilic/hydrophobic segments in the polymer chain. A preliminary study has demonstrated that the catalytic activity of these polymeric organocatalysts are strongly dependent on the aggregated architecture. The micelle-type assemblies can act as nanoreactors to efficiently promote the direct aldolisation of cyclohexanone with aromatic aldehydes in aqueous media, affording anti-aldol products in excellent yields (88–99%) and higher stereoselectivities (90/10 *dr*, 86% *ee*) compared to their nonmicellar systems under identical conditions.

**Keywords:** organocatalysis; micelle; poly(2-oxazoline); asymmetric aldol reaction; pseudopeptide

## 1. Introduction

Since the revival of interest in organocatalysis, the polymeric immobilization of organic catalysts has received considerable research attention as a promising strategy for mimicking enzymatic systems [1–5]. Among the various polymer carriers for loading organocatalysts, the amphiphilic block copolymers are especially attractive as a result of their unique solution properties to associate in both organic and aqueous media to form a range of supramolecular assemblies [6]. By tethering a sort of catalytic entity in the hydrophobic block of the copolymer, the water-compatible catalyst could show a significant improvement in catalytic efficiency by forming specific structures such as micelles. On the other hand, although micellar catalysis in aqueous solution has been known for a long time, polymer-based micelles usually exhibit many advantages over their low-molecular-weight counterparts with respect to structural variability, stability, and functionality [7].

L-Proline and its derivatives, representing the simplest chemical constituents found in type I aldolase enzyme [8], seem to be particularly ideal candidates for the biomimetic design of organocatalysts [9–14]. In this regard, an interesting work recently reported by O'Reilly et al. is the development of a kind of proline-functionalized core-shell micelle for aldol reactions in water [15]. The polymeric nanoparticles showed higher catalytic activity compared to non-supported L-proline, which may be ascribed to the ability of the nanostructures to effectively concentrate the reactants in the catalytically active interior. Based on the thermoresponsive property of multiblock copolymers, they also designed more sophisticated nanoreactors for aqueous asymmetric transformation [16]. In this case, the assembly/disassembly process can be cycled repeatedly just by adjusting temperature below or above the lower critical solution temperature of the shell-forming polymer, which greatly facilitates

catalyst recovery and recycling together with the isolation of pure product. Despite of remarkable advances achieved in the development of water-compatible polymer-supported organocatalysts for aldol reactions [9–11], efficient biomimetic catalytic systems reported thus far remain quite limited. In these catalytic systems, the polymer matrices are mostly confined to styrenics and acrylics [15–20]. Such a polymeric catalyst promoting the asymmetric transformation, although highly desired, may be difficult to mimic an enzymatic environment.

Poly(2-oxazoline)s (POXs) are regarded as analogues of polypeptides because of the intrinsic correlation between the two polymer skeletons, which may have potential for biomedicine-related applications [21–23]. Given their desirable characteristics, such as a great deal of flexibility within molecular design and chemical stability, we recently explored the feasibility of using the unique tertiary amide motif of poly(2-oxazoline)s to covalently immobilize L-proline catalysts. The resultant L-prolinamido-functionalized polymers have proven to be significantly more effective than their monomeric counterparts for the aldolisation of cyclic ketones with several substituted benzaldehydes under neat conditions, indicating that the polymer backbone played an active and synergistic role in the asymmetric transformation mediated by these species [24]. Along with our ongoing interest in the development of pseudopeptide organocatalysts [24,25], in this work, we designed corresponding amphiphilic copolymer versions with the aim of searching for supramolecular micellar catalysis that more closely resembles enzymatic systems. This paper describes the synthesis of both blocky and random copolymers as well as their self-assembly behavior. As a proof-of-concept application, the as-prepared amphiphilic copolymers were used as an organocatalyst for aldol reactions in aqueous media.

## 2. Materials and Methods

### 2.1. Raw Materials and Instruments

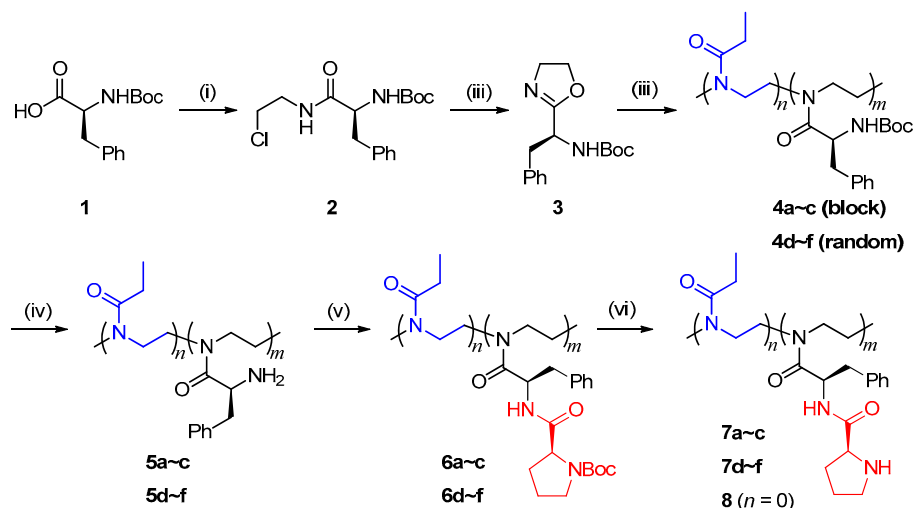
Boc-L-phenylalanine, Boc-L-proline, 2-chloroethylamine hydrochloride, and *O*-(1*H*-benzotriazol-1-yl)-*N,N,N',N'*-tetramethyluronium tetrafluoroborate (TBTU) were purchased from Energy Chemical (Shanghai, China). 2-Ethyl-2-oxazoline (EtOx) was dried and vacuum distilled over barium oxide before use. Dichloromethane (DCM), triethylamine (Et<sub>3</sub>N), and dimethyl sulfoxide (DMSO) were distilled from calcium hydride. Piperidine was dried by sodium hydroxide and distilled to use. Scandium triflate was prepared according to the reported method [26] and stored in a sealed tube. Other chemicals were obtained from Sinopharm Chemical Reagent Co., Ltd. (Shanghai, China) and used as received.

<sup>1</sup>H NMR spectra were recorded on a Bruker Advance DMX400 spectrometer (Bruker Co., Ltd., Karlsruhe, German) with CDCl<sub>3</sub> or DMSO-*d*<sub>6</sub> as the solvent. Chemical shifts were reported in ppm relative to tetramethylsilane (TMS). D-line specific optical rotations ( $[\alpha]_D^{20}$ ) were measured in methanol (10 mg/mL) at 20 °C using a Perkin-Elmer 341 LC polarimeter (Perkin-Elmer Co., Ltd., Waltham, MA, USA). Size exclusion chromatography (SEC) analyses were carried out on a Waters 150C apparatus (Waters Co., Ltd., Milford, MA, USA) equipped with two PLgel 5- $\mu$ m MIXED-C (300 mm  $\times$  7.5 mm) columns (for DMF phase) or Styragel Columns HR4, HR3, and HR1 (for THF phase) and a differential refractometer detector using DMF (flow rate: 1 mL/min, 60 °C) or THF (flow rate: 1 mL/min, 40 °C) as the eluent, respectively. The number-average molecular weight ( $M_n$ ) and polydispersity index ( $\bar{D}$ ) of the polymers were calculated based on PMMA or polystyrene (PS) calibration. High performance liquid chromatography (HPLC) analyses were performed on a Chromeleon apparatus (Dionex Co., Ltd., Sunnyvale, CA, US) equipped with chiral columns (Daicel Chiralpak AD-H, 4.6 mm  $\times$  250 mm) employing *n*-hexane/*i*-PrOH (90/10, *v/v*) as the eluent (flow rate: 0.8 mL/min) and UV detection ( $\lambda = 254$  nm). Dynamic light scattering (DLS) was performed on a Zetasizer Nano Series (Malvern Instruments, Malvern, UK) at 657 nm and a detection angle of 173°. Transmission electron microscopy (TEM) images were captured on a Hitachi HT7700 electron microscope system (Hitachi Co., Ltd., Tokyo, Japan) at an acceleration voltage of 100 kV. An ImageJ software (v 1.51, National Institutes

of Health, Bethesda, MD, USA) was used to label the diameters of 100 randomly selected micelles, and the results are expressed in the form mean  $\pm$  standard deviation.

## 2.2. Synthesis of Polymeric Catalysts

The synthesis of poly(2-oxazoline)-bound L-prolinamide catalysts (L-prolinamido-POXs) is shown in Scheme 1, including synthesis of the functional monomer (S)-2-(1-Boc-amino-2-phenyl)ethyl-2-oxazoline **3** (i–iii), cationic ring-opening copolymerization of **3** with EtOx (iv), and post-modifications towards the precursor polymer **4** (v–vi).



**Scheme 1.** Synthesis of L-prolinamido-poly(2-oxazoline)s. (i)  $\text{ClCH}_2\text{CH}_2\text{NH}_2 \cdot \text{HCl}$ , TBTU,  $\text{Et}_3\text{N}$ , DCM,  $0^\circ\text{C}$ –r.t.; (ii) NaOH, MeOH,  $40^\circ\text{C}$ ; (iii) EtOx,  $\text{Sc}(\text{OTf})_3$ ,  $\text{CH}_3\text{CN}$ ,  $90^\circ\text{C}$ ; (iv) TFA, DCM, r.t.; (v) Boc-L-proline, TBTU,  $\text{Et}_3\text{N}$ , DMSO, r.t.; (vi) TFA, DCM, r.t.

### 2.2.1. (S)-2-(1-Boc-amino-2-phenyl)ethyl-2-oxazoline (**3**)

The monomer was prepared from Boc-L-phenylalanine via two-step reactions in high yield according to the reported method [27]. Boc-L-phenylalanine (20.0 g, 75.4 mmol), 2-chloroethylamine hydrochloride (9.6 g, 82.9 mmol), and TBTU (26.6 g, 82.9 mmol) were dissolved in DCM (200 mL) followed by cooling to  $0^\circ\text{C}$ . Trimethylamine (31.5 mL, 226.2 mmol) was added to the solution dropwise. The mixture was stirred overnight. After removal of the solvent, the resulted residue was purified by silica gel column chromatography with ethyl acetate/petroleum ether (1/2, *v/v*) as the eluent to give product **2** as white solid (22.4 g, 91%).

**2** (20.0 g, 61.2 mmol) was added to methanol solution of NaOH (7.3 g, 183.6 mmol, 250 mL). After stirring for 32 h at  $40^\circ\text{C}$ , the solvent was removed under reduced pressure. The residue was dissolved in DCM (200 mL), washed with deionized (DI) water (200 mL  $\times$  3), dried over  $\text{Na}_2\text{SO}_4$ , filtered, and concentrated under reduced pressure to afford crude product (14.9 g, 84%). Finally, the product (**3**) was purified by recrystallization from EtOAc/hexane. M.p.  $128.5\text{--}129.6^\circ\text{C}$ ;  $[\alpha]_{\text{D}}^{20} = +8^\circ$  (10 mg/mL, MeOH);  $^1\text{H}$  NMR (400 MHz,  $\text{CDCl}_3$ ,  $\delta$ /ppm): 7.36–7.05 (m, 5H), 5.10 (d, 1H), 4.67 (d, 1H), 4.22–4.36 (m, 2H), 3.88–3.69 (m, 2H), 3.09 (ddd, 2H), 1.41 (s, 9H);  $^{13}\text{C}$  NMR (100 MHz,  $\text{CDCl}_3$ ,  $\delta$ /ppm): 167.09 (s), 154.90 (s), 136.31 (s), 129.50 (s), 128.30 (s), 126.79 (s), 79.66 (s), 68.11 (s), 54.09 (s), 49.74 (s), 38.78 (s), 28.31 (s); ESI-MS:  $m/z$  (%) = 290.9 (8.8)  $[\text{M} + \text{H}]^+$ , 312.9 (10)  $[\text{M} + \text{Na}]^+$ , 602.9 (100)  $[2\text{M} + \text{Na}]^+$ . See: Figures S1–S3 in the Supplementary Materials (SM) for NMR and ESI-MS spectra.

### 2.2.2. Cationic Ring-Opening Copolymerization of Monomer **3** and 2-ethyl-2-oxazoline (EtOx)

The general procedure for block-copolymerization (where  $[\mathbf{3}]/[\text{EtOx}]/[\text{I}] = 100/100/1$ ) is described as follows. To a dried flask (Synthware Co., Ltd., Beijing, China) was added monomer **3** (1.20 g, 4.1 mmol) under nitrogen atmosphere. A solution of  $\text{Sc}(\text{OTf})_3$  (2.07 mL, 0.041 mmol) in  $\text{CH}_3\text{CN}$

was added as the initiator. The mixture was heated to 90 °C, stirred for 2 h, and then EtOx was added as the comonomer (0.42 mL, 4.1 mmol). The polymerization was conducted for a further 2 h and terminated by the addition of piperidine (0.10 mL, 1.2 mmol). The resulting solution was concentrated under reduced pressure, dissolved in THF (4 mL), and precipitated out in diethyl ether/*n*-hexane (1/3, *v/v*, 100 mL). The crude product was purified by several dissolution-precipitation processes to give the desired polymer **4b** as a white solid (1.35 g, 83%). The random copolymers were prepared by the same method, in which the monomer mixture was fed at one time.

### 2.2.3. Postmodification of Precursor Polymers

To the mixture of TFA/DCM (1/1, *v/v*, 24 mL) was added **4** (1.20 g, 3.1 mmol) and the resulting solution was stirred for 24 h at room temperature. After removal of the solvent, the residue was dissolved in MeOH (4 mL) and neutralized with saturated NaHCO<sub>3</sub> solution, followed by dialysis against deionized water (*M<sub>w</sub>* cut-off 1000) and lyophilization to afford the deprotected product **5** as a white solid (0.84 g, 90%).

**5** (0.70 g, 2.4 mmol), Boc-L-proline (0.63 g, 2.9 mmol), and TBTU (0.93 g, 2.9 mmol) were dissolved in 200 mL DCM and cooled with an ice bath. To the resulting solution was added Et<sub>3</sub>N (1.0 mL, 7.2 mmol) dropwise and then stirred for 48 h. The mixture was extracted with deionized water (200 mL × 3) and the collected organic phase was concentrated under reduced pressure. The resulting solid was dissolved in a minimum amount of DMF, and an excess amount of hexane was added to precipitate out the desired product **6** (1.1 g, 93%).

**6** (1.00 g, 2.0 mmol) was added into the mixture of TFA/DCM (1/1, *v/v*, 20 mL) and stirred for 24 h at room temperature. After removal of the solvent, the residue was dissolved in MeOH (4 mL) and neutralized with saturated NaHCO<sub>3</sub> solution, followed by dialysis against deionized water (*M<sub>w</sub>* cut-off 1000) and lyophilization to afford the target catalyst **7** as a white solid (0.87 g, 87%).

### 2.3. Micellization of Amphiphilic Copolymers

Polymer micelles were prepared by dialysis according to a generally adapted method [28]. A THF solution of **7** (10 mg/mL) was prepared and dialyzed against deionized water using a dialysis membrane tube (Yuanye biotechnology Co., Ltd., Shanghai, China) with a *M<sub>w</sub>* cut-off of 3500 for 2 days at room temperature. The aqueous micelle solutions were directly used for DLS and TEM measurements and catalytic reactions.

### 2.4. General Procedure for Aldol Reaction

Direct asymmetric aldol reaction of cyclohexanone and *p*-nitrobenzaldehyde was selected as the model reaction. The reactions were carried out under unified and optimized conditions according to our previous studies [24]. To an aqueous solution of catalyst (37.5 μmol in 1 mL DI water, loading 15 mol % of proline groups relative to the aldehyde) was added *p*-nitrobenzaldehyde (0.25 mmol) and cyclohexanone (5 mmol) with rapid stirring to afford emulsion. TFA (1 μL) was added in contrast experiments. The reaction was carried out at 10 °C and monitored by TLC analysis until reaction completion. The mixture was then extracted with ethyl acetate three times. The collected organic phase was dried over Na<sub>2</sub>SO<sub>4</sub>, filtered, and concentrated under reduced pressure. Purification by column chromatography using ethyl acetate and petroleum ether (1/4, *v/v*) as the eluent resulted the aldol product as a pale yellow powder.

## 3. Results and Discussion

### 3.1. Polymerization and Structural Characterization of Polymers

The synthesis of well-defined copolymers **4** is a key step in the preparation of polymeric catalysts. According to our previously reported procedure [29], the ring-opening copolymerization of **3** with

EtOx was allowed to occur in a random or sequential fashion in CH<sub>3</sub>CN using Lewis acidic Sc(OTf)<sub>3</sub> as the initiator.

Table 1 summarizes the polymerization results as well as the copolymer composition, yield, the molar mass, and its polydispersity index ( $\bar{D}$ ). Under optimal conditions, copolymers having a controlled molecular weight and relatively narrow polydispersity ( $\bar{D} = 1.33$ – $1.45$ ) could be obtained in moderate to high yield. However, the yield decreased by increasing the content of **3** in the monomer feed in either sequential or random copolymerization (entries 1–3 and 4–6). Meanwhile, the copolymer composition deviated slightly from the theoretical values at a higher monomer/initiator ratio. In all the experiments, SEC analyses gave unimodal molar mass distributions for the resultant polymers (Figure S4 in SM). The ring-opening copolymerization was achieved in a controllable fashion, as previously reported [24,28,29].

**Table 1.** Copolymerization results of **3** with 2-ethyl-2-oxazoline (EtOx) initiated with Sc(OTf)<sub>3</sub><sup>1</sup>.

Entry	Feed Ratio [ <b>3</b> ]/[EtOx]/[I]	Poly- <b>3</b>			Copolymer <b>4</b>			
		$M_n$ <sup>2</sup>	$\bar{D}$ <sup>2</sup>	Code	$M_n$ <sup>2</sup>	$\bar{D}$ <sup>2</sup>	Yield (%) <sup>3</sup>	<b>3</b> (mol%) <sup>4</sup>
1	50/150/1	4900	1.19	<b>4a</b>	8700	1.33	90	25
2	100/100/1	7800	1.25	<b>4b</b>	11,400	1.38	83	50
3	150/50/1	11,600	1.34	<b>4c</b>	14,000	1.45	60	80
4	50/150/1	-	-	<b>4d</b>	9900	1.34	96	25
5	100/100/1	-	-	<b>4e</b>	10,700	1.37	91	47
6	150/50/1	-	-	<b>4f</b>	10,800	1.33	80	71

<sup>1</sup> [M] = 2 mol/L, 90 °C; Entries 1–3 and 4–6 for block and random copolymerization, respectively; see: Experimental section. <sup>2</sup> Determined by SEC with PMMA calibration, DMF as the eluent;  $\bar{D} = M_w/M_n$ . <sup>3</sup> Isolated yield. <sup>4</sup> Calculated by <sup>1</sup>H NMR (CDCl<sub>3</sub>).

On the other hand, the monomer reactivity ratios of **3** and EtOx were determined to be 0.044 and 2.832, respectively. The measurements were conducted according to the Fineman–Ross (FR) method [30] (see Figure S5 and Table S1 in SM). Apparently, regarding the reactivity of both monomers, it is justified to reason that their polymerization proceeds with a much different rate. Figure 1 plots, as an example, the changes in molar fraction ( $f_1$ ) of **3** in the copolymers as a function of monomer conversion, which clearly demonstrated the formation of gradient copolymers instead of strictly statistical copolymers in the abovementioned random copolymerization. This was also confirmed indirectly by their self-assembly behavior in water (vide infra).

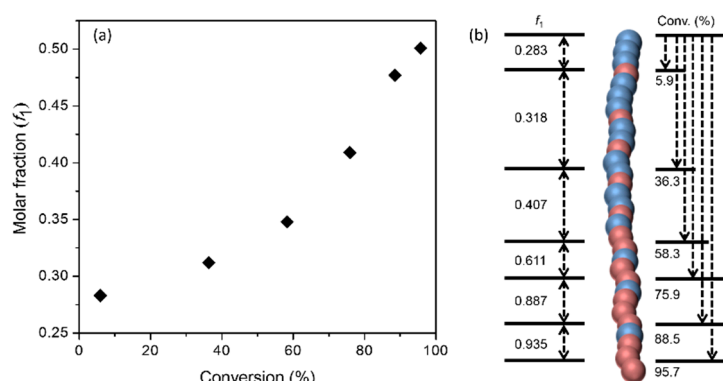


**Figure 1.** (a) Molar fraction ( $f_1$ ) of **3** in the copolymers vs. monomer conversion and (b) schematic representation of gradient polymer structures. Copolymerization: [I]:[**3**]:[EtOx] = 1:50:50; the monomer conversion was monitored with <sup>1</sup>H NMR spectroscopy.

### 3.2. Postmodification of Copolymer 4

$^1\text{H}$  NMR spectroscopy was employed to track the postmodification process of the precursor polymers **4**. As an example, Figure 2a,d compares  $^1\text{H}$  NMR spectra of the polymer **4b** and its derivatives **5b**, **6b**, and **7b**, all of which show the characteristic signals of the methane proton ( $d$ – $e$ ) of the main chains around 3.4 ppm. The signal of Boc groups, observed for **4b** in Figure 2a at 1.25 ppm, disappeared fully in the spectrum of **5b** (Figure 2b), and a weak band ( $a$ ) centered at  $\sim 8.6$  ppm from the protonated amine groups concomitantly appeared, indicating that deprotection was achieved. In Figure 2c, **6b** showed  $^1\text{H}$  NMR signals arising from pyrrolidinyl moieties at 4.0 ( $j$ ), 2.0–1.5 ( $k$ ,  $l$ ) and  $\sim 2.8$  ppm ( $m$ ) as well as those due to Boc protons at 1.44–1.06 ppm ( $n$ ), which confirm the cooperation of the prolinamide moieties. Calculated from the relative integration values, i.e., “ $n$ ” vs. “ $i$ ” in Figure 2c and “ $h$ ” vs. “ $i$ ” in Figure 2a, the *L*-proline functionalization (the grafting efficiency) was estimated to be more than 90% in the preparation of **6a–e** (see Table 2). As evidenced by Figure 2d from the absence of a peak at  $\sim 1.25$  ppm that is characteristic of Boc groups, the deprotection was almost quantitatively completed, giving the corresponding polymeric catalysts with different unit ratios in good yields ( $>85\%$ ). It is worth mentioning that the signal from amide N–H was not detected as a consequence of the proton exchange with trace water in the deuterated solvent [31,32].

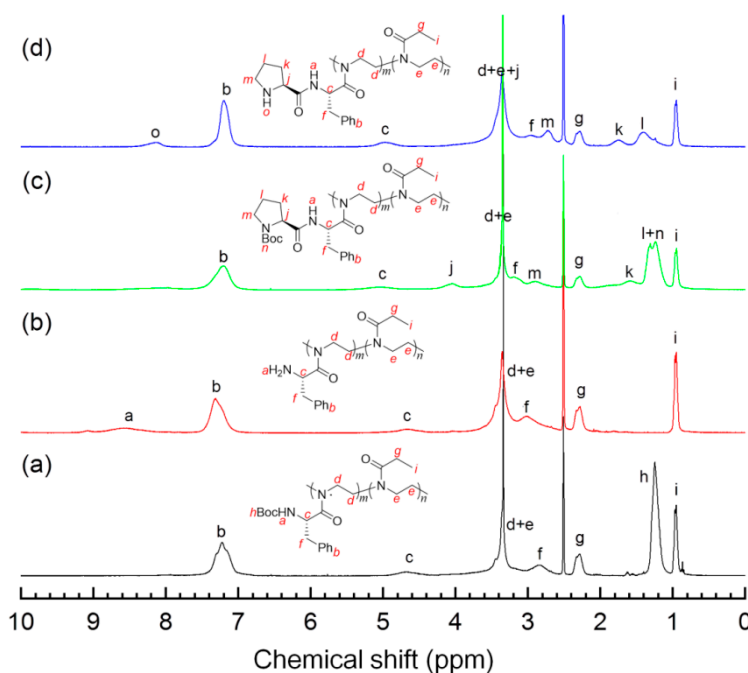


**Figure 2.**  $^1\text{H}$  NMR spectra (DMSO- $d_6$ , 400 MHz) of the copolymers collected at different reaction stages: (a) **4b**, (b) **5b**, (c) **6b**, and (d) **7b**.

**Table 2.** SEC characterization results of the copolymer **6**.

Entry	Code	$M_n$ <sup>1</sup>	$\bar{D}$ <sup>1</sup>	$E_f$ (%) <sup>2</sup>
1	<b>6a</b>	6600	1.30	98
2	<b>6b</b>	8700	1.39	97
3	<b>6c</b>	10,000	1.54	90
4	<b>6d</b>	8200	1.23	97
5	<b>6e</b>	9600	1.27	95
6	<b>6f</b>	11,900	1.30	91

<sup>1</sup> PMMA calibration, DMF as the eluent. <sup>2</sup> Calculated by  $^1\text{H}$  NMR (CDCl<sub>3</sub>).

Another point which should be noted is that the polymeric catalysts **7** were not suitable for SEC measurements due to their strong interaction with column fillers [28]. Therefore, the molecular weights of **7** were indirectly characterized in their Boc-protected form (i.e., **6**). As seen from Table 2, all the *N*-Boc-prolinamide derivatives except for **6f** showed lower  $M_n$  values than the corresponding precursors (**4**) of the same copolymer composition when compared pairwise, which might be attributed to their different hydrodynamic properties. However, the polydispersity indices of the two were similar.

### 3.3. Self-Assembly Behavior of Polymer **7** in Water

After removing the Boc-group from **6**, all the deprotected products (copolymers **7**) showed good water solubility, and the Tyndall effect could be observed in the aqueous solution. The combination of DLS and TEM measurements on these systems revealed that the colloidal dispersions consisted of particles of tens to hundreds of nanometers, depending on the ratio of hydrophilic/hydrophobic segments and their distribution in the polymer chain. For example, from Figure 3a,c the intensity-average hydrodynamic diameter ( $D_h$ ) was 35 nm and 304 nm for the block copolymer **7c** and its random counterpart **7f**, respectively. Correspondingly, the TEM images showed the present morphologies of presumably spherical aggregates with diameters of about 30 and 310 nm. Taking into account both the hydration degree and the polydispersity effects, the mean particle sizes estimated by TEM compared reasonably well to the average  $D_h$ s. It is worth noting, however, that the gradient copolymer **7f** seemed to self-assemble into large compound aggregates induced by inter/intrapolymer hydrogen bonding, which is similar to those reported in the literature [33,34]. Furthermore, for the polymer **7f**, the lack of a suitable hydrophilic–hydrophobic balance most likely led to the formation of a large number of small-sized assemblies during dialysis. From TEM observations of **7f** self-assembling in THF/H<sub>2</sub>O (Figure 3d), these small sphere-like particles adhere to the surface of large aggregates or exist in a free state.

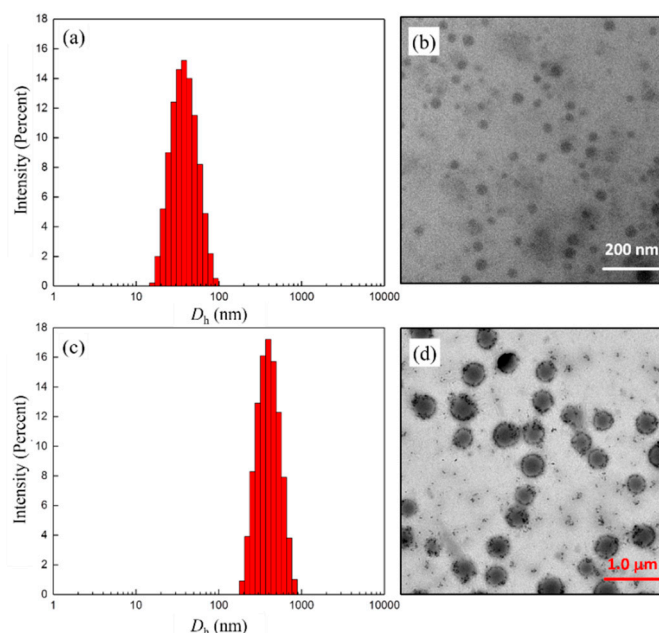


**Figure 3.** DLS results and TEM images obtained from aqueous solutions of copolymers **7c** (a,b) and **7f** (c,d), respectively. Sample conc. = 1 mg/mL.

For the block copolymers, the average  $D_h$  value undergoes a significant decrease from 212 (**7a**) to 35 nm (**7c**) when the molar ratio of the hydrophobic segment increases from 25% to 80%, which is in line with the general rule of amphiphilic assemblies [6]. In contrast, the aggregates formed from the gradient copolymers **7d–f** showed much larger  $D_h$ s (304–426 nm) than that of the corresponding block copolymers with similar composition and grafting percentage (see Table 3, **7a** vs. **7d**, **7b** vs.

**7e**, and **7c** vs. **7f**). This result indicated that the hydrophilic/hydrophobic ratio and its distribution in the main chain played a key role in the formation of self-assembling nanostructures. In fact, the amphiphilic block copolymers (**7a**) with high EtOx content (>50 mol%) exhibited a weak tendency to self-assemble, so it was hard to get high-quality TEM images for its aqueous solution (see Figure S6). As for the homopolymer **8**, it was not suited for water-phase DLS and TEM measurements due to its hydrophobicity.

**Table 3.** Results of DLS and TEM measurements of **7**.

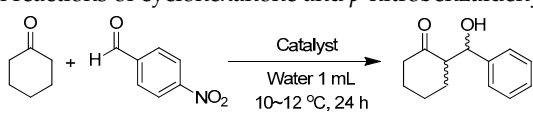
Entry	Code	DLS		TEM
		$D_h$ (nm) <sup>1</sup>	PDI <sup>1</sup>	Size (nm) <sup>2</sup>
1	<b>7a</b>	212	0.259	190 ± 60
2	<b>7b</b>	85	0.330	60 ± 20
3	<b>7c</b>	35	0.112	30 ± 10
4	<b>7d</b>	426	0.198	380 ± 60
5	<b>7e</b>	376	0.182	330 ± 60
6	<b>7f</b>	304	0.085	310 ± 70

<sup>1</sup>  $c = 1$  mg/mL, DI water, 10 °C. <sup>2</sup> The statistical size was calculated from TEM images of **7a–f** (as shown in Figure 3 and Figure S6). All the samples were prepared from 1 mg/mL micelle aqueous solutions.

### 3.4. Evaluation of Catalytic Activity

The aldol reaction of *p*-nitrobenzaldehyde with cyclohexanone was employed as a benchmark test of the polymeric catalysts (Table 4), as frequently reported in the literature [35–38]. In the absence of an acidic additive, the reaction proceeded smoothly in water, affording aldol products in 24 h with excellent yield (85–96%) and moderate to good diastereoselectivity (71:29–90:10 anti:syn ratio). Comparable enantioselectivity was observed for the antiproduct in the reactions using the blocky and random copolymer catalysts (58–70% *ee*) with the exception of **7d** (31% *ee*, entry 7). Upon addition of TFA, which has often been used as an acidic additive to improve catalytic efficiency in many organocatalytic transformations [39–41], all catalysts gave aldol products in better yield (90–99%) with higher enantioselectivities ranging from 71% to 86%. More importantly, the *ee* value improved from 71% for the block copolymer **7a** to 77% for **7b** and to 86% for **7c** (entries 2, 4, and 6). In other words, the trend of enantioselectivity enhancement corresponded well to a hydrodynamic diameter decrease from 212 to 35 nm (entries 1–3 in Table 3). A similar tendency in enantioselectivity was observed in the case without TFA (entries 1, 3, and 5 in Table 4). However, the random copolymers, or more strictly, gradient copolymers **7d–f**, did not seem to follow this general rule. In this case, the *ee* values were almost the same (80–82%) for the copolymers with different hydrophilic/hydrophobic ratios, although a higher enantioselectivity was achieved with TFA compared to the systems without the acidic additive (entries 7–12).

Overall, the stereoselectivity of the block copolymer **7c** was superior to that of **7f** and the homopolymer **8** and their activities were comparable (see entries 6, 13, and 14 in Table 4). The higher catalytic efficiency of **7c** with respect to its analogues (**7a**, **7b**, or **7d–f**) might be explained by the relatively small particle size of ~30 nm. The polymer chains tucked in the micellar interior was expected to establish a microenvironment favorable for strengthening the interaction between the catalytic sites and reactants, thus leading to a higher catalytic activity and to higher levels of stereocontrol in the aqueous media [42]. As demonstrated in light scattering experiments, upon introduction of reactants, an increase in micelle sizes was observed, suggesting that the hydrophobic substrates are concentrated in the catalytically active inner core, and the nanostructure was not destroyed even in the case of TFA being added (Figure S7).

**Table 4.** Aldol reactions of cyclohexanone and *p*-nitrobenzaldehyde in water <sup>1</sup>.


Entry	Catalyst	TFA (μL)	Yield (%) <sup>2</sup>	anti/syn <sup>3</sup>	ee (%) <sup>4</sup>
1	7a	0	85	86/14	58
2	7a	1	90	83/17	71
3	7b	0	96	87/13	63
4	7b	1	99	88/12	77
5	7c	0	93	87/13	67
6	7c	1	96	90/10	86
7	7d	0	94	71/29	31
8	7d	1	91	81/19	82
9	7e	0	89	86/14	70
10	7e	1	93	87/13	82
11	7f	0	91	77/23	65
12	7f	1	96	83/17	80
13	8 <sup>5</sup>	0	97	77/23	52
14	8 <sup>5</sup>	1	96	81/19	80

<sup>1</sup> Reaction was performed in a mixture of deionized (DI) water (1 mL), *p*-nitrobenzaldehyde (0.25 mmol), and cyclohexanone (5 mmol) in the presence of 37.5 μmol catalyst (based on the actual concentration of proline groups, 15 mol% relative to the aldehyde). The data in the table are the average of three parallel experiments, and the error is controlled within 5%. <sup>2</sup> Isolated yield. <sup>3</sup> Diastereomeric ratio, determined by <sup>1</sup>H NMR (CDCl<sub>3</sub>). <sup>4</sup> Determined by HPLC with chiral column (Figure S8); the absolute configuration of the products was deduced by comparing the retention time with reported values [43–45]. <sup>5</sup>  $M_n \approx 5800$ ,  $M_w/M_n = 1.28$  [24].

#### 4. Conclusions

In summary, a class of amphiphilic poly(2-oxazoline) derivatives bearing a L-prolinamide pendant was synthesized by the combination of controlled cationic ring-opening polymerization and a postmodification strategy. Upon direct dissolution in water, the copolymers self-assembled into micelle-type aggregates with particle sizes of tens to hundreds of nanometers depending on the different hydrophilic/hydrophobic ratios and their distribution in the main chain. In the aldol reaction of cyclohexanone with *p*-nitrobenzaldehyde proceeded in aqueous media, the block copolymer catalyst **7c** gave optimal results in terms of both the yield (up to 99%) and stereoselectivity (90/10 *dr*, 86% *ee*), pointing to the existence of a fortunate micellar effect. Although the polymer-based micellar catalyst presents some limitations and more work remains to be done to improve activity and stereoselectivity, this study provides a new design strategy based on the pseudopeptide scaffolds for biomimetic catalytic systems.

**Supplementary Materials:** The following are available online at <http://www.mdpi.com/2073-4360/10/9/1004/s1>, Figure S1: <sup>1</sup>H NMR spectrum of **3** (CDCl<sub>3</sub>, 400 MHz), Figure S2: <sup>13</sup>C NMR spectrum of **3** (CDCl<sub>3</sub>, 101 MHz), Figure S3: ESI-MS of **3**, Figure S4: SEC curves of diblock copolymers (a) and random copolymers (b), Figure S5: FR plot for the copolymerization of **3** and EtOx at low conversion, Figure S6: TEM images of aqueous solutions of **7a**, **7b**, **7d**, and **7e**; see Table 3, Figure S7: DLS results of **7c** aq. solution (1 mg/mL) before and after addition of (a) cyclohexanone (~0.2 mg/mL) and (b) TFA (1 μL/mL), Figure S8: A representative HPLC analysis of the aldol products. Mobile phase: *n*-hexane: *i*PrOH = 1:9, 0.8 mL/min, Table S1: FR parameters for copolymerization of **3** with EtOx at low conversion <sup>a</sup>.

**Author Contributions:** Conceptualization, L.J. and K.L.; Methodology, Y.W.; Validation, K.L., L.Y., and L.J.; Formal Analysis, L.Y.; Investigation, K.L. and Y.W.; Resources, L.J.; Data Curation, Y.W.; Writing-Original Draft Preparation, K.L. and L.Y.; Writing-Review & Editing, L.J.; Visualization, G.D.; Supervision, L.J.; Project Administration, L.J.; Funding Acquisition, L.J.

**Funding:** The authors are very grateful to the National Natural Science Foundation of China (Grant No. 21474089, 21274122) for financial support.

**Conflicts of Interest:** The authors declare no conflict of interest. The funders had no role in the design of the study; in the collection, analyses, or interpretation of data; in the writing of the manuscript, and in the decision to publish the results.

## References

1. Benaglia, M.; Puglisi, A.; Cozzi, F. Polymer-supported organic catalysts. *Chem. Rev.* **2003**, *103*, 3401–3430. [[CrossRef](#)] [[PubMed](#)]
2. Cozzi, F. Immobilization of organic catalysts: when, why, and how. *Adv. Synth. Catal.* **2006**, *348*, 1367–1390. [[CrossRef](#)]
3. Gruttadauria, M.; Giacalone, F.; Noto, R. Supported proline and proline-derivatives as recyclable organocatalysts. *Chem. Soc. Rev.* **2008**, *37*, 1666–1688. [[CrossRef](#)] [[PubMed](#)]
4. Yin, Y.; Dong, Z.; Luo, Q.; Liu, J. Biomimetic catalysts designed on macromolecular scaffolds. *Prog. Polym. Sci.* **2012**, *37*, 1476–1509. [[CrossRef](#)]
5. Breslow, R.; Bandyopadhyay, S.; Levine, M.; Zhou, W. Water exclusion and enantioselectivity in catalysis. *ChemBioChem* **2006**, *7*, 1491–1496. [[CrossRef](#)] [[PubMed](#)]
6. Wang, J.; Liu, K.; Xing, R.R.; Yan, X.H. Peptide self-assembly: thermodynamics and kinetics. *Chem. Soc. Rev.* **2016**, *45*, 5589–5604. [[CrossRef](#)] [[PubMed](#)]
7. Torchilin, V.P. Structure and design of polymeric surfactant-based drug delivery systems. *J. Controlled Release* **2001**, *73*, 137–172. [[CrossRef](#)]
8. Wong, C.H.; Halcomb, R.L.; Ichikawa, Y.; Kajimoto, T. Enzymes in organic synthesis: application to the problems of carbohydrate recognition (part 1). *Angew. Chem. Int. Ed.* **1995**, *34*, 412–432. [[CrossRef](#)]
9. Gruttadauria, M.; Giacalone, F.; Marculescu, A.M.; Lo Meo, P.; Riela, S.; Noto, R. Hydrophobically directed aldol reactions: polystyrene-supported L-proline as a recyclable catalyst for direct asymmetric aldol reactions in the presence of water. *Eur. J. Org. Chem.* **2007**, *28*, 4688–4698. [[CrossRef](#)]
10. Benaglia, M.; Celentano, G.; Cozzi, F. Enantioselective aldol condensations catalyzed by poly(ethylene glycol)-supported proline. *Adv. Synth. Catal.* **2001**, *343*, 171–173. [[CrossRef](#)]
11. Benaglia, M.; Cinquini, M.; Cozzi, F.; Puglisi, A.; Celentano, G. Poly(ethylene glycol)-supported proline: a versatile catalyst for the enantioselective aldol and iminoaldol reactions. *Adv. Synth. Catal.* **2002**, *344*, 533–542. [[CrossRef](#)]
12. Huerta, E.; Stals, P.J.; Meijer, E.W.; Palmans, A.R.A. Consequences of folding a water-soluble polymer around an organocatalyst. *Angew. Chem. Int. Ed.* **2013**, *52*, 2906–2910. [[CrossRef](#)] [[PubMed](#)]
13. Lu, A.; Moatsuo, D.; Longbottom, D.A.; O'Reilly, R.K. Tuning the catalytic activity of L-proline functionalized hydrophobic nanogel particles in water. *Chem. Sci.* **2013**, *4*, 965–969. [[CrossRef](#)]
14. Kehat, T.; Goren, K.; Portnoy, M. Effects of dendritic interface on enantioselective catalysis by polymer-bound prolines. *New J. Chem.* **2012**, *36*, 394–401. [[CrossRef](#)]
15. Lu, A.; Cotanda, P.; Patterson, J.P.; Longbottom, D.A.; O'Reilly, R.K. Aldol reactions catalyzed by L-proline functionalized polymeric nanoreactors in water. *Chem. Commun.* **2012**, *48*, 9699–9701. [[CrossRef](#)] [[PubMed](#)]
16. Zayas, H.A.; Lu, A.; Valade, D.; Amir, F.; Jia, Z.; O'Reilly, R.K.; Monteiro, M.J. Thermoresponsive polymer-supported L-proline micelle catalysts for the direct asymmetric aldol reaction in water. *ACS Macro Lett.* **2013**, *2*, 327–331. [[CrossRef](#)]
17. Guo, G.; Wu, Y.; Zhao, X.; Wang, J.; Zhang, L.; Cui, Y. Polymerization of L-proline functionalized styrene and its catalytic performance as a supported organocatalyst for direct enantioselective aldol reaction. *Tetrahedron Asymmetry* **2016**, *27*, 740–746. [[CrossRef](#)]
18. Arakawa, Y.; Wennemers, H. Enamine catalysis in flow with an immobilized peptidic catalyst. *ChemSusChem* **2013**, *6*, 242–245. [[CrossRef](#)] [[PubMed](#)]
19. Doyagüez, E.G.; Parra, F.; Corrales, G.; Fernández-Mayoralas, A.; Gallardo, A. New hydroxyproline based methacrylic polybetaines: Synthesis, pH sensitivity and catalytic activity. *Polymer* **2009**, *50*, 4438–4446. [[CrossRef](#)]
20. Uemukai, T.; Ishifune, M. Synthesis and catalytic activity of the thermoresponsive polymers having pyrrolidine side chains as base functionalities. *J. Appl. Polym. Sci.* **2013**, *127*, 2554–2560. [[CrossRef](#)]
21. Wilson, P.; Ke, P.C.; Davis, T.P.; Kempe, K. Poly(2-oxazoline)-based micro- and nanoparticles: A review. *Eur. Polym. J.* **2017**, *88*, 486–515. [[CrossRef](#)]
22. Hoogenboom, R. Poly(2-oxazoline)s: A polymer class with numerous potential applications. *Angew. Chem. Int. Ed.* **2009**, *48*, 7978–7994. [[CrossRef](#)] [[PubMed](#)]
23. Luxenhofer, R.; Han, Y.; Schulz, A.; Tong, J.; He, Z.; Kabanov, A.V.; Jordan, R. Poly(2-oxazoline)s as polymer therapeutics. *Macromol. Rapid. Commun.* **2012**, *33*, 1613–1631. [[CrossRef](#)] [[PubMed](#)]

24. Wang, Y.; Shen, H.; Zhou, L.; Hu, F.; Xie, S.; Jiang, L. Novel poly(2-oxazoline)s with pendant L-prolinamide moieties as efficient organocatalysts for direct asymmetric aldol reaction. *Catal. Sci. Technol.* **2016**, *6*, 6739–6749. [[CrossRef](#)]
25. Hu, F.; Du, G.; Ye, L.; Zhu, Y.; Wang, Y.; Jiang, L. Novel amphiphilic poly(2-oxazoline)s bearing L-prolinamide moieties as the pendants: Synthesis, micellization and catalytic activity in aqueous aldol reaction. *Polymer* **2016**, *102*, 33–42. [[CrossRef](#)]
26. Kobayashi, S.; Hachiya, I. Lanthanide triflates as water-tolerant Lewis acids. Activation of commercial formaldehyde solution and use in the aldol reaction of silyl enol ethers with aldehydes in aqueous media. *J. Org. Chem.* **1994**, *59*, 3590–3596. [[CrossRef](#)]
27. Engelhardt, N.; Weberskirch, R. Synthesis and characterization of surface functional polymer nanoparticles by a bottom-up approach from tailor-made amphiphilic block copolymers. *Macromol. Chem. Phys.* **2013**, *214*, 2783–2791. [[CrossRef](#)]
28. Vlasi, E.; Papagiannopoulos, A.; Pispas, S. Amphiphilic poly(2-oxazoline) copolymers as self-assembled carriers for drug delivery applications. *Eur. Polym. J.* **2017**, *88*, 516–523. [[CrossRef](#)]
29. Hu, F.; Xie, S.; Jiang, L.; Shen, Z. Living cationic ring-opening polymerization of 2-oxazolines initiated by rare-earth metal triflates. *RSC Adv.* **2014**, *4*, 59917–59926. [[CrossRef](#)]
30. Fineman, M.; Ross, S.D. Linear method for determining monomer reactivity ratios in copolymerization. *J. Polym. Sci.* **1950**, *5*, 259–262. [[CrossRef](#)]
31. Lee, J.S.; Regatte, R.R.; Jerschow, A. Bloch equations for proton exchange reactions in an aqueous solution. *Concepts Magn. Reson. Part A* **2016**, *45A*, e21397. [[CrossRef](#)] [[PubMed](#)]
32. Craven, C.J.; Derix, N.M.; Hendriks, J.; Boelens, R.; Hellingwerf, K.J.; Kaptein, R. Probing the nature of the blue-shifted intermediate of photoactive yellowprotein in solution by NMR: Hydrogen–deuterium exchange data and pH studies. *Biochemistry* **2000**, *39*, 14392–14399. [[CrossRef](#)] [[PubMed](#)]
33. Zhu, Y.; Liu, L.; Du, J. Probing into homopolymer self-assembly: how does hydrogen bonding influence morphology? *Macromolecules* **2012**, *46*, 194–203. [[CrossRef](#)]
34. Feng, C.; Lu, G.; Li, Y.; Huang, X. Self-assembly of amphiphilic homopolymers bearing ferrocene and carboxyl functionalities: Effect of polymer concentration,  $\beta$ -cyclodextrin, and length of alkyl linker. *Langmuir* **2013**, *29*, 10922–10931. [[CrossRef](#)] [[PubMed](#)]
35. Zhang, D.; Ren, C.; Yang, W.; Deng, J. Helical polymer as mimetic enzyme catalyzing asymmetric aldol reaction. *Macromol. Rapid Commun.* **2012**, *33*, 652–657. [[CrossRef](#)] [[PubMed](#)]
36. Huerta, E.; van Genabeek, B.; Stals, P.J.M.; Meijer, E.W.; Palmans, A.R.A. A modular approach to introduce function into single-chain polymeric nanoparticles. *Macromol. Rapid Commun.* **2014**, *35*, 1320–1325. [[CrossRef](#)] [[PubMed](#)]
37. Yeh, C.; Sun, Y.R.; Huang, S.J.; Tsai, Y.M.; Cheng, S. Alternating chiral selectivity of aldol reactions under the confined space of mesoporous silica. *Chem. Commun.* **2015**, *51*, 17116–17119. [[CrossRef](#)] [[PubMed](#)]
38. Deng, J.; Deng, J. Optically active microspheres from helical substituted polyacetylene with pendent ferrocenyl amino-acid derivative. Preparation and recycling use for direct asymmetric aldol reaction in water. *Polymer* **2017**, *125*, 200–207. [[CrossRef](#)]
39. Chen, F.; Huang, S.; Zhang, H.; Liu, F.; Peng, Y. Proline-based dipeptides with two amide units as organocatalyst for the asymmetric aldol reaction of cyclohexanone with aldehydes. *Tetrahedron* **2008**, *64*, 9585–9591. [[CrossRef](#)]
40. Miura, T.; Imai, K.; Ina, M.; Tada, N.; Imai, N.; Itoh, A. Direct asymmetric aldol reaction with recyclable fluorinated organocatalyst. *Org. Lett.* **2010**, *12*, 1620–1623. [[CrossRef](#)] [[PubMed](#)]
41. de Arriba, Á.L.F.; Simon, L.; Raposo, C.; Alcazar, V.; Sanz, F.; Muniz, F.M.; Moran, J.R. Imidazolidinone intermediates in prolinamide-catalyzed aldol reactions. *Org. Biomol. Chem.* **2010**, *8*, 2979–2985. [[CrossRef](#)] [[PubMed](#)]
42. Duss, M.; Manni, L.S.; Moser, L.; Handschin, S.; Mezzenga, R.; Jessen, H.J.; Landau, E.M. Lipidic mesophases as novel nanoreactor scaffolds for organocatalysts: Heterogeneously catalyzed asymmetric aldol reactions in confined water. *ACS Appl. Mater. Inter.* **2018**, *10*, 5114–5124. [[CrossRef](#)] [[PubMed](#)]
43. Lei, M.; Shi, L.; Li, G.; Chen, S.; Fang, W.; Ge, Z.; Cheng, T.; Li, R. Dipeptide-catalyzed direct asymmetric aldol reactions in the presence of water. *Tetrahedron* **2007**, *63*, 7892–7898. [[CrossRef](#)]

44. Hernández, J.G.; Juaristi, E. Asymmetric aldol reaction organocatalyzed by (S)-proline-containing dipeptides: improved stereinduction under solvent-free conditions. *J. Org. Chem.* **2011**, *76*, 1464–1467. [[CrossRef](#)] [[PubMed](#)]
45. Bayat, S.; Tejo, B.A.; Salleh, A.B.; Abdulmalek, E.; Yahya, N.M.; Rahman, M.B.A. Various polar tripeptides as asymmetric organocatalyst in direct aldol reactions in aqueous media. *Chirality* **2013**, *25*, 726–734. [[CrossRef](#)] [[PubMed](#)]



© 2018 by the authors. Licensee MDPI, Basel, Switzerland. This article is an open access article distributed under the terms and conditions of the Creative Commons Attribution (CC BY) license (<http://creativecommons.org/licenses/by/4.0/>).